Electrostastic Control of Spontaneous Curvature in Catanionic Reverse Micelles

ARTICLE *in* LANGMUIR · OCTOBER 2007

Impact Factor: 4.46 · DOI: 10.1021/la7016038 · Source: PubMed

Electrostastic Control of Spontaneous Curvature in Catanionic Reverse Micelles

Benjamin Abécassis,*,†,‡ Fabienne Testard,*,† Lise Arleth,§ Steen Hansen,§ Isabelle Grillo,|| and Thomas Zemb†

LIONS - CEA Saclay, 91191 Gif-Sur-Yvette, France, University of Copenhagen, Faculty of Life Sciences, Department of Natural Sciences, Thorvaldsensvej 40, DK-1871 Frederiksberg C, Denmark, and Institut Laue-Langevin, DS/LSS, 6 rue Jules Horowitz, B.P. 156, 38042 Grenoble, France

Received June 4, 2007. In Final Form: July 10, 2007

By means of small-angle neutron scattering and conductivity measurements, we study the microstructure of octylammoniumoctanoate/octane/water catanionic reverse microemulsions with an excess of anionic or cationic surfactant. Increasing the surface charge makes the microemulsion able to incorporate much more water than in the neutral case, up to 10 water molecules per surfactant. Even with charges in the surfactant film, wormlike micelles are present in the microemulsion domain. Along water dilution lines, the classical rod-to-sphere transition due to the minimization of the curvature energy of the rigid surfactant film is observed. When temperature is decreased, a re-entrant phase transition associated with the liquid−gas equilibrium of attractive cylinders is observed. Using the framework of the Tlusty−Safran theory, attraction could originate from junctions between wormlike reverse micelles. In any case, the spontaneous curvature of the catanionic surfactant film depends on both the temperature and the net charge, whatever the sign of the latter.

1. Introduction

Catanionic surfactants are mixtures of an anionic and a cationic surfactant.[1] The main feature of these systems is that the charge of the surfactant film can be varied by changing the proportion between the two surfactants.[2] They can be classified into two categories: the first one is true catanionics when surfactants are mixed in acid and hydroxide forms and no salt from the initial counterions is present.[3,4] The second and most frequently studied category is when counterions are present. This last case induces complex systems as, for example, when mixed surfactants are in a sodium and bromide form where at least five components are present. In water, these surfactants self-assemble into original microstructures that strongly depend on the stoichiometry between the positive and negative moieties. For example, micrometer icosahedra are obtained when an excess of anionic surfactant is used[5] whereas disks are more stable for a positively charged bilayer. This general structural sequence can be explained by the intrinsic stiffness of the catanionic bilayer in water.[6,7] Few studies in the literature assess the behavior of catanionic surfactants in nonaqueous media. Jokela et al.[8] described, in their pioneering study, the extension of the reverse microemulsion domain in the phase diagram of the octylammonium−octanoate/water/octane system. These reverse microemulsions can also be obtained with catanionic surfactants with shorter alkyl chains.[9,10] Kunieda et al. reviewed[11] the third phase behavior and solubilization properties of microemulsions made of catanionic surfactants and alcohol. Despite these studies of phase diagrams and some applications of catanionic reverse micelles in nanoparticles synthesis[12−15] or enzymatic reaction,[16] nearly no information is available on the structure of reverse catanionic microemulsions.

In a previous article,[17] the ternary system octylammoniumoctanoate/octane/water in the oil corner of the phase diagram was revisited by means of scattering techniques and conductivity. The combination of those techniques enabled us to shed light on the topology of the microemulsion. As the water-to-surfactant ratio increases, the reverse micelles grow uniaxially into first short rodlike micelles and then into long wormlike micelles. Strong 1D growth is also observed when the overall surfactant concentration increases for a fixed water-to-surfactant ratio (R_w) or if the temperature decreases toward the lower phase boundary of the one-phase system. Junctions or van der Waals attraction between cylinders through oil[18] can be at the origin of an effective attraction that eventually leads, at low temperature, to a phase separation between a dilute and a concentrated phase containing the same type of aggregates. For a neutral catanionic monolayer,

* Corresponding authors. E-mail: benjamin.abecassis@gmail.com, fabienne.testard@cea.fr.

† LIONS - CEA Saclay.

‡ Present adress: LPMCN, Université de Lyon 1 and Physico-Chimie Théorique, ESPCI, France.

§ University of Copenhagen.

|| Institut Laue-Langevin.

(1) Khan, A.; Marques, E. In *Specialist Surfactant*; Robb, I., Ed.; Blackie Academic and Professional: London, 1997; Chapter 3.

(2) Jokela, P.; Jonsson, B.; Khan, A. *J. Phys. Chem.* **1987**, *91*, 3291−3298.

(3) Zemb, T.; Dubois, M. *Aust. J. Chem.* **2003**, *56*, 971−979.

(4) Zemb, Th.; Carrière, D.; Glinel, K.; Hartmann, M.; Meister, A.; Vautrin, Cl.; Delorme, N.; Fery, A.; Dubois, M. *Colloids Surf., A* **2007**, *303*, 37−45.

(5) Dubois, M.; Deme, B.; Gulik-Krzywicki, T.; Dedieu, J. C.; Vautrin, C.; Desert, S.; Perez, E.; Zemb, T. *Nature (London)* **2001**, *411*, 672−675.

(6) Zemb, T.; Dubois, M.; Deme, B.; Gulik-Krzywicki, T. *Science* **1999**, *283*, 816−819.

(7) Dubois, M.; Lizunov, V.; Meister, A.; Gulik-Krzywicki, T.; Verbavatz, J. M.; Perez, E.; Zimmerberg, J.; Zemb, T. *Proc. Natl. Acad. Sci. U.S.A.* **2004**, *101*, 15082−15087.

(8) Jokela, P.; Jonsson, B.; Eichmuller, B.; Fontell, K. *Langmuir* **1988**, *4*, 187−192.

(9) Khan, a.; Mendonca, C. *J. Colloid Interface Sci.* **1995**, *169*, 60−64.

(10) Friman, R.; Backlund, S.; Hognesen, E.; Austad, T. *Tenside, Surfactants, Deterg.* **2004**, *41*, 190−194.

(11) Li, X.; Kunieda, H. *Curr. Opin. Colloid Interface Sci.* **2003**, *8*, 327−336.

(12) Shi, H. T.; Qi, L. M.; Ma, J. M.; Cheng, H. M. *Chem. Commun.* **2002**, 1704−1705.

(13) Shi, H. T.; Qi, L. M.; Ma, J. M.; Cheng, H. M.; Zhu, B. Y. *Adv. Mater.* **2003**, *15*, 1647−1651.

(14) Shi, H. T.; Qi, L. M.; Ma, J. M.; Wu, N. Z. *Adv. Funct. Mater.* **2005**, *15*, 442−450.

(15) Shi, H. T.; Wang, X. H.; Zhao, N. N.; Qi, L. M.; Ma, J. M. *J. Phys. Chem. B* **2006**, *110*, 748−753.

(16) Mahiuddin, S.; Renoncourt, A.; Bauduin, P.; Touraud, D.; Kunz, W. *Curr. Opin. Colloid Interface Sci.* **2004**, *9*, 43−47.

(17) Abécassis, B.; Testard, F.; Arleth, L.; Hansen, S.; Grillo, I.; Zemb, T. *Langmuir* **2006**, *22*, 8017−8028.

(18) Parsegian, A. *van der Waals Forces*; Cambridge University Press: 2005.

10.1021/la7016038 CCC: $37.00
Published on Web 08/21/2007

this rich polymorphism was explained by the variation of spontaneous curvature with temperature varying in the same way as for other nonionic surfactants[20] (i.e., the curvature decreases with decreasing the temperature, with the convention of a positive curvature toward water). In nonionic surfactant microemulsions, spontaneous curvature is controlled by temperature, and thus the microstructure is profoundly influenced by temperature. In catanionic microemulsions, the charge of the interface can be controlled by the relative stoichiometry of the pair of ionic surfactants used, and this should impact the variation of spontaneous curvature and thus the structure of the reverse microemulsion.

In the present article, we therefore investigate the microstructure and phase behavior of the reverse catanionic microemulsions of octylammoniumoctanoate/octane/water for a nonstoichiometric ratio of anionic and cationic components. This is achieved by changing the amine-to-acid ratio using the carboxylate or the ammonium salt. Jokela and co-workers[8] have shown that the addition of sodium octanoate (which makes the interface negatively charged) leads to an important increase in the extent of the reverse microemulsion region. By means of conductivity measurements and scattering techniques, we study the influence of surface charge on the topology of the reverse microemulsion. Our findings are discussed in the framework of theories on microemulsion.

2. Experimental Section

Unless otherwise stated, all of the experiments were conducted at 25 °C.

2.1. Chemicals. Octanoic acid (99.5%), octylamine (99%), octane (99%), and sodium octanoate (99%) were purchased from Sigma-Aldrich. Octylamine hydrochloride (99%) was purchased from Acros Organics. They were all used as received. Deuterated octane (98%) was purchased from Eurisotop (France). Deionized water obtained from a Milli-Q purification system (Millipore) with a resistivity of 18.2 MΩ·cm was used to prepare samples.

2.2. Sample Preparation. The catanionic surfactant was obtained by mixing equal quantities of octanoic acid and octylamine in diethylether followed by the evaporation of solvent under vacuum, which finally gives a white powder. To prepare a microemulsion, given quantities of (deuterated) octane, water, catanionic surfactant, and excess charged surfactant (either sodium octanoate or octylamine hydrochloride) were weighed in a Teflon screw cap vial and vortex mixed. A clear, low-viscosity solution was obtained. For conductivity measurements, hydrogenated octane was used. For the SANS experiments, deuterated octane was used, and the catanionic surfactant and water were hydrogenated compounds. The phase boundaries were slightly different when either deuterated or hydrogenated solvents were used, but the general phase behavior remains unchanged. A microemulsion can be completely defined by three parameters: the overall surfactant concentration (denoted as c), the water-to-surfactant ratio (denoted as R_w), and the ratio between anionic and catanionic surfactants (denoted as r_c).

$$r_c = \frac{[\text{C8COOH}] + [\text{C8COONa}]}{[\text{C8COOH}] + [\text{C8COONa}] + [\text{C8NH2}] + [\text{C8NHCl}]}$$

The compositions of the different samples are indicated in Table 1.

2.3. Conductivity Measurements. Conductivity measurements were performed using a Mettler DL77 titrator coupled to a Tacussel CD810 conductimeter. Small amounts of water were automatically added to a given microemulsion under magnetic agitation. The time between the addition of water and the measurement was 1 min. To ensure that no kinetic artifacts perturb the measurement, several microemulsions of different water-to-surfactant ratios were prepared and equilibrated for 1 day before the conductivity measurement is performed. The difference in conductivity between the two methods was within the precision of the conductimeter.

Table 1. Composition of the Different Samples Studied[a]

concentration (mol·L^{-1})	R_w	r_c	volumic fraction	max $p(r)$
0.8	2.1	0.55	0.143	25.5
0.8	3.2	0.55	0.153	32.3
0.8	8.6	0.55	0.200	36
0.4	5.7	0.45	0.087	35
0.4	7.7	0.45	0.096	38
0.4	8.7	0.45	0.100	43
0.4	10.1	0.45	0.106	40

[a] The volumetric fraction is relative to the overall volume of reverse micelles (water and surfactant).

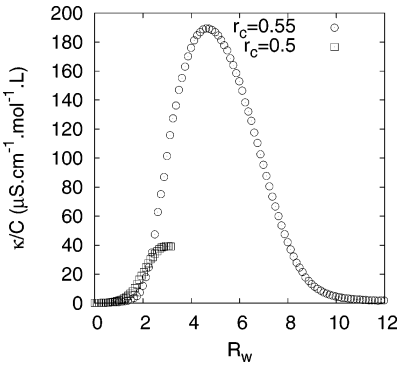

Figure 1. Normalized conductivity along the water dilution line for $c = 0.8$ M and two different r_c values in the L2 phase. A single microemulsion phase is present all along this dilution line

2.4. Small-Angle Neutron Scattering. Small-angle neutron scattering (SANS) measurements were performed on the D22 instrument at the ILL (Institut Laue Langevin, Grenoble, France). Three different combinations of collimation lengths and sample to detector distances were used in order to cover a wide range of scattering vectors and to get sufficient overlap between the data set from the different configurations. The scattering diagrams were then radially averaged and put on an absolute scale using ILL standard procedures. The microemulsions were transferred in Helma cells (1 or 2 mm thick) and placed in a thermostatted sample holder.

The SANS data were analyzed using the same methods and models as described in our previous article.[17] A slightly modified version of the indirect Fourier transform[19,21] was used in the initial data analysis to convert the experimental scattering intensity, $I(q)$, to a direct space representation in terms of the pair-distance distribution function, $p(r)$. In the next step, the previously described[17] model fitting approach was used where models for spherical droplets, short cylindrical micelles, and long wormlike micelles were fitted to the experimental data. This was done to investigate which model gives the most representative description and to extract more quantitative structural information than can be obtained from an inspection of the $p(r)$ functions.

3. Results

Figure 1 presents the behavior of conductivity in the reverse microemulsion of the octylammoniumoctanoate/octane/water system upon increasing the water to surfactant ratio at $c = 0.8$ M, for excess of negative charge ($r_c = 0.55$), and for the neutral case ($r_c = 0.5$). The net charge of the surfactant film is equal to 5.2 μC·cm^{-2} (or 3.2×10^{-3} e·Å^{-2}) for $r_c = 0.55$. In this case, a minimal quantity of water, corresponding to $R_w = 0.8$ in the case of $c = 0.8$ M, is necessary to get a clear microemulsion without any trace of excess insoluble solid (with dry sodium

(19) Glatter, O. *J. Appl. Crystallogr.* **1977**, *10*, 415−421.
(20) Strey, R. *Colloid Polym. Sci.* **1994**, *272*, 1005
(21) Hansen, S. *J. Appl. Cryst.* **2000**, *33*, 1415−1421.

octanoate being insoluble in octane). The microemulsion region is greatly extended toward higher values of the water-to-surfactant ratio as compared to the neutral case. The maximum R_w at which excess water is expelled from the microemulsion (i.e., at the emulsification failure) is 12, to be compared to 3.3 in the neutral case. As previously shown by Jokela et al.,[22] when charges are present at the interface, the system tends to be stabilized with larger amount of water.

Conductivity along the water dilution line in the domain of reverse micelles can be used to follow the variation in the structure of the microemulsion. As shown in Figure 1, charging the interface strongly influences the conductivity. For $r_c = 0.55$, the conductivity increases, reaches a maximum, and then decreases by more than 1 order of magnitude to reach almost the conductivity of pure octane just before the emulsification failure. Typical electric antipercolation is observed (i.e., a decrease in conductivity by orders of magnitude upon addition of water for a given surfactant concentration). Antipercolation was first observed in charged w/o microemulsions by Kaler and co-workers[23] and was also observed to be dependent on the penetrating power of oil in reverse microemulsions of DDAB/water/alkane.[24] The antipercolation phenomena rely on a rod-to-sphere transition at constant curvature and is rationalized by the DOC model[25] for reverse microemulsions with a stiff interface. This antipercolation is thus predicted in the framework of the DOC model consisting of cylinders connected by spherical junctions.

In the present system, this transition is also evidenced by SANS experiments performed on the same dilution line and is shown in Figure 2.

The first two samples ($R_w = 2.1$ and 3.2) are located before the maximum of the conductivity versus R_w curves as shown in Figure 1. The "tails" at high r values of the obtained $p(r)$ functions indicate that long rodlike or wormlike micelles are formed. This analysis is confirmed by the results of model-based analysis (fit results in Figure 2): for the $R_w = 2.1$ sample, a good fit to the SANS data is obtained with a model for wormlike micelles with an elliptical cross section. The elliptical micellar cross section has a minor axis of $R_{minor} = 13$ Å and a major axis of $R_{major} = 19$ Å. The length of the micelles is (at least) $L = 800$ Å, and the Kuhn length is $b = 150$ Å. These parameters show that the micelle structure is similar to those found in the neutral system.[17] For the $R_w = 3.2$ sample, the best fit is still obtained with the wormlike micelle model. In this case, we get $R_{minor} = 17$ Å, $R_{major} = 27$ Å, $L = 600$ Å, and $b \approx 600$ Å. Thus, we obtain considerably thicker and more rigid rodlike micelles than in the $R_w = 2.1$ case. It must be noted here that a water-to-surfactant ratio of less than 6 means a strong reduction in water activity and molecular volume, and the Kuhn length can increase with the diameter because there is no free water in the system. However, the quality of the fit of the $R_w = 3.2$ data is not as good as in the $R_w = 2.1$ case. This might be the result of the coexistence of long wormlike micelles and spherical microemulsion droplets formed upon further addition of water to the system (discussed below). In the $R_w = 8.6$ sample, the forward scattering is lower than for $R_w = 2.1$ and 3.2, and the power-law behavior at low q has disappeared. In the corresponding $p(r)$ function, the tails observed at high r values in the $R_w = 2.1$ and 3.2 samples have also disappeared (Figure 2). These data thus indicate the formation of spherical micelles or droplets interacting via a short-range

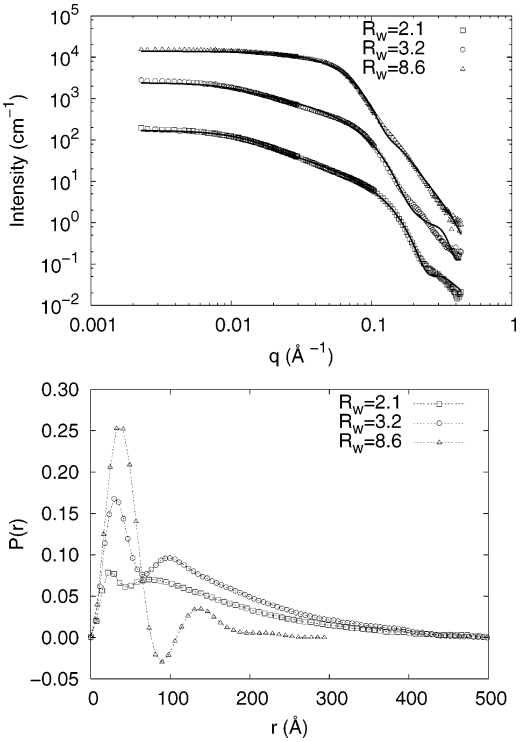

Figure 2. SANS diagram and PDDF obtained along the water dilution line for $c = 0.8$ M and $r_c = 0.55$. The $R_w = 3.2$ and 8.6 sample intensities have been multiplied by 10 and 100, respectively, for clarity.

repulsion (as stated by the depletion just after the maximum at 65 Å corresponding to the sphere diameter). These conclusions are in agreement with the model-based analysis where good fits to the experimental data can be obtained with a model for polydisperse spherical droplets with an average radius of $R_{av} = 35$ Å and a relative standard deviation $\sigma/R_{av} = 0.20$ (using a Gaussian size distribution as explained in ref 17). These data are thus consistent with the conductivity measurements and show that upon addition of water the shapes evolve gradually from rodlike objects to globular, roughly spherical aggregates under the constraint of curvature.

For the neutral case,[17] we showed the large effect of temperature on the topology of the microemulsion. The attraction between connected cylinders, either due to connection points or to van der Waals attraction between polar cores, is able to drive a liquid−gas phase separation between two distinct L_2 phases separated by a meniscus. This behavior is ubiquitous for microemulsions: there are tie lines between the concentrate and dilute microemulsions in the phase diagram, which is close to a single-phase microemulsion.[26] It is the second type of phase instability observed in microemulsions, with the first one being the emulsification failure. To test the effect of temperature when charges are present at the interface, conductivity measurements were performed at 15 °C as shown in Figure 3.

As in the 25 °C case, a small amount of water is necessary to get a microemulsion from the pure surfactant/solvent solution. Upon addition of water, the conductivity increases, and phase separation occurs at $R_w = 2.5$. Two microemulsions coexist, with the denser one containing almost all of the water. The volume of the dense phase increases with the water-to-surfactant ratio. At $R_w = 6.1$, the two phases remix to give a single-phase microemulsion of high conductivity. At this point, adding further

(22) Jonsson, B.; Jokela, P.; Lindman, B.; Sadaghiani, A. *Langmuir* **1991**, *7*, 889−895.
(23) Rushforthy, D. S.; Sanchez-Rubio, M.; Santos-Vidal, L. M.; Wormuth, K. R.; Kaler, E. W.; Cuevas, R.; Puig, J. *J. Phys. Chem.* **1986**, *90*, 6668.
(24) Chen, S.; Evans, D.; Ninham, B. *J. Phys. Chem.* **1984**, *88*, 1631.
(25) Zemb, T. *Colloids Surf., A.* **1997**, *129−130*, 435−454.
(26) Chevalier, Y.; Zemb, T. *Rep. Prog. Phys.* **1990**, *53*, 279−371.

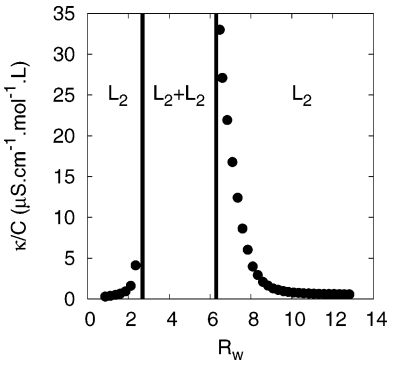

Figure 3. Normalized conductivity along the water dilution line for $c = 0.4$ M and $r_c = 0.55$. Measurements are conducted at 15 °C. An $L_2 + L'_2$ phase transition is observed during the addition of water.

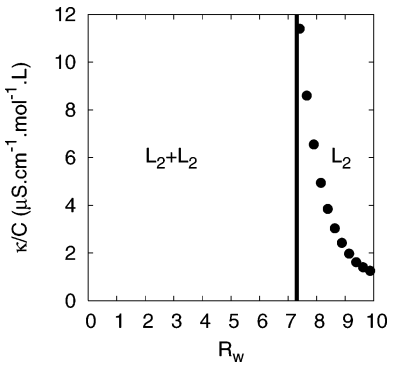

Figure 4. Normalized conductivity along the water dilution line for $c = 0.8$ M and $r_c = 0.45$. Measurements are obtained at 25 °C.

inner phase makes the conductivity decrease, and the antipercolation phenomenon that is observed at 25 °C remains unchanged. The nature of the phase separation must be the same as that observed with decreasing temperature in the neutral case. For low R_w values, a sphere-to-rod transition is driven by the amount of water. The effective attractions that can occur only between rods induces liquid−liquid phase separation between two w/o microemulsions: a concentrate and a dilute one.

To test the symmetry of the behavior toward the sign of the charge, the sodium carboxylate is changed to an ammonium chloride. For $r_c = 0.45$, the complete dissolution of the excess charged surfactant also necessitates a certain amount of water. At 25 °C, the first solution without any trace of solid is biphasic, and no single microemulsion phase is present before phase separation. The biphasic system is an equilibrium between two microemulsions. Upon increasing the amount of water, a single phase is obtained, and an antipercolation is retrieved as in the $r_c = 0.55$ case (Figure 4).

The small-angle neutron scattering experiments are also consistent with a transition from (connected) wormlike micelles to spherical droplets (Figure 5). At the lowest R_w value ($R_w = 5.7$), very long wormlike micelles are formed. From the model fits, we obtained $R_{minor} = 16$ Å, $R_{major} = 26$ Å, $L \approx 5000$ Å, and $b \approx 200$ Å. Upon addition of water, the correlations at long distances disappear as stated in the scattering-intensity data by the disappearance of the power-law behavior at low q and are more directly seen in the $p(r)$ function where the dominant tails at large r values disappear. In the samples with $R_w = 7.7$, 8.7, and 10.1, the signature of rodlike or wormlike micelles has totally disappeared. Instead, the pair-distance distribution functions indicate that spherical droplets are formed. However, the second maximum of the $p(r)$ functions around 150 Å indicates that the droplets are somewhat sticky and that a small dimer population

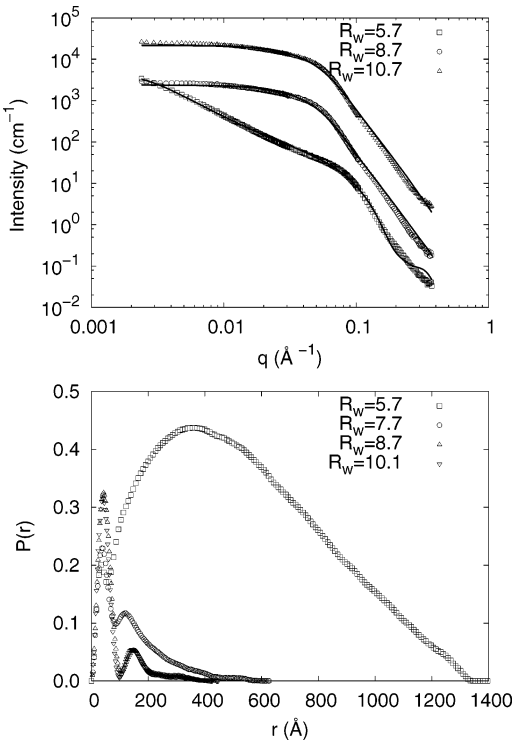

Figure 5. SANS diagram and PDDF obtained along the water dilution line for $c = 0.4$ M and $r_c = 0.45$. The $R_w = 8.7$ and 10.7 sample intensities have been multiplied by 10 and 100, respectively, for clarity.

is present.[27] Reasonable model fits could be obtained to the $R_w = 8.7$ and 10.1 data. For the $R_w = 8.7$ sample, we found an R_{av} of 38 Å and a relative standard deviation $\sigma/R_{av} = 0.39$ whereas for the $R_w = 10.1$ sample we found an R_{av} of 35 Å with $\sigma/R_{av} = 0.41$. However, the fit quality was not excellent in either one of these cases, most likely because the droplet−droplet attractions indicated by the $p(r)$ functions were not taken into account in the model-based analysis. For the $R_w = 7.7$ sample, none of the applied simple models gave satisfactory fits to the experimental data. This sample may have an intermediate structure containing a mixture of wormlike micelle and droplet structures. This coexistence is clearly visible in some direct systems as shown by Talmon et al.[28] or by Lin[29] using cryo-TEM.

The addition of charges, either positive or negative, thus has the same effect on the behavior of the microemulsion. The network region is extended, eventually leading to $L_2 + L'_2$ phase separation depending on the temperature and the concentration. This phase separation (when it occurs) is followed (with increasing R_w) by a remixing of the phases into a single microemulsion and an antipercolation phenomenon leading to a pure phase of spheres before emulsification failure is observed. The only differences when negative charges are replaced by positive ones concern the concentration and temperature limits for the transitions. These differences can be explained by the fact that ammonium is a strong base and carboxylate is a weak acid, a property that introduces some differences in electrostatic repulsion between catanionic surfactant films.[30] Moreover, the volume and the area per polar head are different for the anionic and cationic species.

(27) Glatter, O. In *Neutrons, X-rays, and Light: Scattering Methods Applied to Soft Condensed Matter*; Lindner, P., Zemb, T., Eds.; Elsevier: Amsterdam, 2002.

(28) Bernheim-Groswasser, A.; Watchel, E.; Talmon, Y. *Langmuir* **2000**, *16*, 4131−4140.

(29) Lin, Z. *Langmuir* **1996**, 1729−1737.

(30) Meister, A.; Dubois, M.; Belloni, L.; Zemb, T. *Langmuir* **2003**, *19*, 7259−7263.

4. Discussion

The microstructure and properties of a microemulsion are directly linked to the properties of the surfactant film that separates water and oil. If the thermal fluctuations are neglected, then the bending energy of the film depends on the spontaneous curvature ($c_0 = \rho_0^{-1}$), the cross section of the micelles (R), which is directly proportional to R_w, and the elastic constants of the surfactant film (κ and $\bar{\kappa}$).[31] The spontaneous curvature and elastic constants of the film are also related to the molecular details of the different constituants of the microemulsion through the packing parameter concept.[32] The minimization of the bending energy of the film in correlation with the geometrical constraints thus dictates the structure (shape, global features) and instabilities of the microemulsion. We adopt the convention of counting curvature toward water as positive. For a given constant spontaneous curvature with a negative Gaussian modulus, cylinders are preferred for small inner phase contents.[33,34] Upon increasing the water-to-surfactant ratio, the most stable topology consists of a network of interconnected rods, and finally spheres become more stable. For the emulsification failure, a pure phase of disconnected spheres is present in the solution in coexistence with pure water. Emulsification failure of cylinders or network could be predicted only when thermal fluctuations are taken into account.[31] The octylammoniumoctanoate/octane/water reverse microemulsions present different topologies and different emulsification failures of spheres and cylinders depending on the charge of the surfactant film.

We demonstrated in a previous paper[17] that for the neutral case of octylammoniumoctanoate/octane/water reverse microemulsion, as the water to surfactant ratio increases the micelles grow uniaxially into first short rodlike micelles and second into long wormlike micelles. For a negative net charge of the film, experiments demonstrate here the presence of reverse cylindrical micelles at low R_w values. As the water-to-surfactant ratio increases, the micelles grow uniaxially into long wormlike micelles before antipercolation occurs. The conductivity measurements and the corresponding SANS data unambiguously show that along a water dilution line, a phase of connected cylinders is followed by a phase of disconnected spheres. This antipercolation is a general feature observed for all water-in-oil microemulsions with a stiff interface, with stiff meaning here that bending constants are larger than kT.[35,36] This antipercolation phenomenon has to rely on changes in the topology of the microemulsion upon increasing the water content. Along the water dilution line, the only geometrical possibility upon increasing the water content (i.e., the volume-to-surface ratio at constant curvature) is to go to a rod-to-sphere transition[6] with the rod radius roughly equal to two-thirds of the radius of the final spheres.[32] The DOC model[32] is based on a generalized connected structure that locally satisfies three constraints: the volume fraction, the specific surface, and the curvature or its microscopic translation packing parameter P, which are good approximations for all stiff microemulsions. This model allows us to derive the antipercolation lines of electric conductivity under strong constraints in phase diagrams from spontaneous curvature, expressed in terms of packing parameter P or the reverse.[6]

The major difference observed between the neutral and charged cases is that antipercolation cannot be observed in the neutral case as a result of emulsification failure, which occurs before this transition. As shown in the previous paper,[17] for $r_c = 0.5$, the emulsification failure occurs for small R_w between a network of connected cylinders and nearly pure water (typical values are below 4). Large differences in the spontaneous curvature when charges are present can explain this difference. Hence, the extension of the microemulsion domain is strongly dependent on the charge of the surfactant film. The addition of a significant charge decreases the value of the spontaneous curvature, and emulsification failure occurs for a higher water content. Considering the water core, the electrostatic repulsions decrease upon increasing the radius of the reverse micelles. The distance between the excess charges of the same sign increases while the water content is increased. This qualitatively explains the decrease in spontaneous curvature when increasing the surface charge of the micelles.

For small R_w values, wormlike micelles are obtained in the neutral and charged cases as supported by conductivity and SANS results in the low-R_w region. In the present system, in both cases (neutral and charged) and opposite to the known reverse microemulsion lecithin/water/octane, no macroscopic gel is observed in the solutions. This can be a strong indication of branching of the wormlike micelles with the connection point sliding along the cylinders. It is known that a nonviscous solution is obtained for branching wormlike micelles whereas unconnected cylinders produce extremely viscous microemulsions.[37,38] Considering the presence of junctions in the reverse catanionic microemulsion allows one to explain the variation of the phase diagram with temperature and water content. At low temperature, an L_2/L'_2 phase separation is observed either for the neutral case[17] or with excess charges (Figures 3 and 4). This phase separation between concentrate and dilute microemulsion phases is due to attraction between reverse micelles. The attraction originates from van der Waals forces between aqueous cores of the micelles or from the formation of connection points (junctions) between wormlike micelles acting as an effective attraction. For the neutral case,[17] the liquid−gas phase separation is attributed in part to the presence of junctions, which are more numerous when the temperature decreases because of a decrease in spontaneous curvature with temperature.[17] This re-entrant phase separation is captured by the Tlusty−Safran theory.[39] In the case of a microemulsion that adopts the topology of a branched network, the effective intermicellar attraction is governed by the free energies required to form a junction and an end cap. The energy of a junction depends nonmonotically on the radius of the cylinders, which is proportional to R_w, and is given by[40]

$$\epsilon(r,T) \simeq \frac{\kappa(T)}{T}\epsilon_0\left[1 + \epsilon_2\left(c_0\rho - \frac{1}{2}\right)^2\right] \qquad (1)$$

where $\epsilon_0 \simeq 2$ and $\epsilon_2 \simeq 10$. A deep minimum is present at $c_0\rho = 1/2$ and corresponds to a steep maximum in effective attraction between junctions (magnitude proportional to $\exp(-\epsilon(r,T)/kT)$, after which end caps and hence disconnected cylinders are more

(31) Safran, S.; Turkevich, L. *Phys. Rev. Lett.* **1983**, *50*, 1930−1933.
(32) Ninham, B.; Barnes, I.; Hyde, S.; Derian, P.; Zemb, T. *Europhys. Lett.* **1987**, *4*, 561−568.
(33) Safran, S.; Turkevich, L.; Pincus, P. *J. Phys. (Paris), Lett.* **1984**, *45*, 19.
(34) Hyde, S.; Andersson, S.; Larsson, K.; Blum, Z.; Landh, T.; Lidin, S.; Ninham, B. *The Language of Shape: The Role of Curvature in Condensed Matter−Physics, Chemistry, and Biology;* Elsevier: Amsterdam, 1996; pp 170−176.
(35) Barnes, I.; Derian, P.; Hyde, S.; Ninham, B.; Zemb, T. *J. Phys. France* **1990**, *51*, 2605−2628.
(36) Barnes, I.; Hyde, S.; Ninham, B.; Derian, P.; Drifford, M.; Zemb, T. *J. Phys. Chem* **1988**, *92*, 2286−2293.
(37) Cates, M.; Candau, S. *J. Phys.: Condens. Matter* **1990**, *2*, 6869−6892.
(38) Khatory, A.; Kern, F.; Lequeux, F.; Appell, J.; Porte, G.; Morie, N.; Ott, A.; Urbach, W. *Langmuir* **1993**, 933−939.
(39) Tlusty, T.; Safran, S.; R., S. *Phys. Rev. Lett.* **2000**, *84*, 1244−1247.
(40) Tlusty, T.; Safran, S.; Menes, R.; Strey, R. *Phys. Rev. Lett.* **1997**, *78*, 2616−2619.

likely. Thus, for water-in-oil microemulsions, the effective attraction between the junctions exhibits a maximum for a given R_w value. Increasing R_w from zero to this maximum increases the effective attraction, leading the system to a phase separation. A further increase in water content decreases the attraction, hence entropy tends to remix the phases. The effective attraction created by the junctions is balanced by two terms that are dependent only on the volume fraction (and not on the tube radius): the hard sphere repulsion and the restriction of thermal fluctuations of the tubes. When these two repulsions are sufficient, no phase separation occurs, and a single microemulsion phase is present. This is observed for $c = 0.8$ M and $r_c = 0.55$ at $T = 25$ °C as shown in Figure 1, in which a topological rod-to-sphere transition is observed. When the attraction is too strong, phase separation occurs with increasing R_w as shown in Figure 3 for $c = 0.4$ M and $r_c = 0.55$ at $T = 15$ °C.

The conductivity variation along with water content described in Figure 3 is clearly supported using the Tlusty−Safran theory. First, we observe a single microemulsion phase at a low water-to-surfactant ratio. With increasing water composition, the micelles grow, and the junctions appear as stated by the increase in the conductivity. When the density of junctions reaches a certain point, $L_2 + L'_2$ phase separation is observed at $R_w = 2.4$. As stated before, the energy of a junction is a nonmonotonic function of the water-to-surfactant ratio, hence upon increasing the content of the inner phase, after the maximum junction density is reached, attraction decreases and remixing of the two phases occurs at $R_w = 6.2$. Similar behavior is observed when octylamine hydrochloride is added instead of sodium octanoate (corresponding to $r_c = 0.45$), but the major difference is the temperature at which phase separation occurs. As shown in Figure 5, for $T = 25$ °C the first microemulsion region is not present, and phase separation occurs directly when the amount of water is high enough to solubilize the excess charged surfactant. With increasing water content, a single reverse microemulsion is obtained at $R_w = 7.3$ with an antipercolation phenomena. The SANS correlated to the conductivity measurement supports the fact that a rod-to-sphere transition is also observed for a positively charged film.

The behavior of a catanionic reverse microemulsion is thus "symmetric" toward the change in sign of the structural charge of the catanionic surfactant film and can be summarized by Figure 6. This diagram was first derived by Menes et al.[41] using a mean-field approach that considers a microemulsion with attractive interactions. The qualitative behavior is not changed by the nature of the attraction involved and rationalizes all of the features observed in the studied catanionic reverse microemulsions with variations in charge, temperature, and water content.

For a given concentration, when no charges are present, a single-phase microemulsion is observed, and emulsification failure occurs for a connected reverse cylinder phase. When the surface charge is increased, the spontaneous radius of curvature increases, and the horizontal line of constant spontaneous radius of curvature cuts the region where two microemulsions are in equilibrium. When $r_c = 0.45$ at $T = 25$ °C, phase separation is observed whereas a single phase is observed for $r_c = 0.5$ and 0.55. This shows that the extent of the increase in the spontaneous radius of curvature is more important when the interface is positively charged by the cationic excess surfactant. On the microscopic scale, this difference shall be explained by a difference in the preferred packing parameter of the two surfactants (charge density and area per polar head). This shift toward smaller spontaneous curvature (higher spontaneous radius of curvature) can also be obtained by decreasing the temperature, but the extent to which this variation can occur is much higher when playing on the charge. If the emulsification failure line does not intercept the two-phase region and if the spontaneous curvature is sufficiently small to authorize spheres to be stable, then the network-to-sphere transition occurs in the single microemulsion region, and we do not observe the $L_2 + L'_2$ phase separation as observed for $c = 0.8$ M and $r_c = 0.55$. The two-phase region is shifted toward higher values of the spontaneous radius of curvature if the volume fraction is increased as the steric repulsion acts against the attraction created by the junctions.

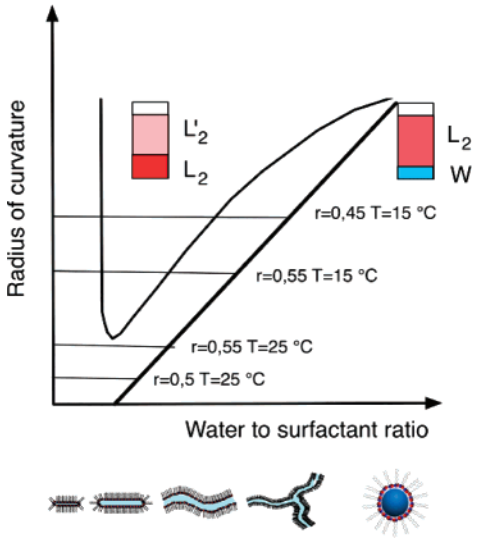

Figure 6. Qualitative phase diagram (inspired by ref 41) representing the stable phases depending on the spontaneous radius of curvature and the water-to-surfactant ratio for a given volume fraction

In summary, at constant spontaneous curvature, we always observe the same succession of shapes by tuning the water-to-surfactant ratio. Depending on the spontaneous curvature, the two-phase instabilities (emulsification failure and liquid−gas transition) can occur for different values of water-to-surfactant ratios. We have shown that both the temperature and the surface charge can precisely tune the spontaneous curvature and that all of the features observed can be explained by this fine control over the preferred curvature of the surfactant film. Finally, the rheological behavior of these systems would be worth investigating. A quantitative study of the viscosity of these microemulsions as a function of the different parameters could yield an interesting link between the microstructure and this macroscopic quantity.

5. Conclusions

The influence of a slight amount of excess charge versus electroneutrality on catanionic microemulsions is crucial. When an excess of one of the two components is present, the electrostatic repulsion between the charges makes the microemulsion region broader as compared to the neutral case. Hence, the spontaneous curvature of the surfactant film can be tuned by this means and provides efficient control over the topology and phase behavior of these systems, but the physics of the system is not changed and is still governed by the curvature of the rigid surfactant film. Rodlike long reverse micelles are present, and along a water dilution line, the classical rod-to-sphere transition is observed. With decreasing temperature, a re-entrant phase transition associated with a dilute/concentrate phase separation is observed. This re-entrant phase transition could originate from an effective attraction mediated by junctions between cylindrical micelles as

(41) Menes, R.; Safran, S.; Strey, R. *Phys. Rev. Lett.* **1995**, *74*, 3399−3402.

suggested by Tlusty et al.[40] The temperature of this transition is strongly dependent on the surface charge of the film, which tunes the spontaneous curvature. As for nonionic systems, the spontaneous curvature varies with temperature. In the catanionic case, the surface charge is another way to tune this parameter that has not yet been reported.

Acknowledgment. We thank Julie Goyon for experimental help, Grégoire Porte, Michel Delsanti, and Luc Belloni for fruitful discussions, and the Institut Laue-Langevin for the provision of beam time.

LA7016038